Acta Pharmaceutica Sinica B 2017;7(2):230–240

Chinese Pharmaceutical Association
Institute of Materia Medica, Chinese Academy of Medical Sciences

Acta Pharmaceutica Sinica B

www.elsevier.com/locate/apsb
www.sciencedirect.com

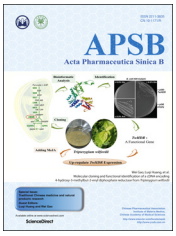

ORIGINAL ARTICLE

Synthesis, characterization and pharmacological evaluation of pyrazolyl urea derivatives as potential anti-inflammatory agents

Kanagasabai Somakala, Mohammad Amir*

Department of Pharmaceutical Chemistry, Faculty of Pharmacy, Hamdard University, New Delhi 110062, India

Received 8 June 2016; revised 5 July 2016; accepted 17 July 2016

KEY WORDS

Pyrazolyl urea;
p38;
MAPK;
DPPH;
Anti-inflammatory;
Gastric toxicity;
Lipid peroxidation

Abstract p38α mitogen activated protein kinase (MAPK) inhibitors provide a novel approach for the treatment of inflammatory disorders. A series of fifteen pyrazolyl urea derivatives (**3a–o**) were synthesized and evaluated for their p38α MAPK inhibition and antioxidant potential. Compounds **3a–e, 3g** and **3h** showed low micromolar range potency (IC_{50} values ranging from 0.037 $\pm$ 1.56 to 0.069 $\pm$ 0.07 μmol/L) compared to the standard inhibitor SB 203580 (IC_{50} = 0.043 $\pm$ 3.62 μmol/L) when evaluated for p38α MAPK inhibition by an immunosorbent-based assay. Antioxidant activity was measured by a 2,2′-diphenyl-1-picryl hydrazyl radical (DPPH) free radical scavenging method and one of the compounds, **3c**, showed better percentage antioxidant activity (75.06%) compared to butylated hydroxy anisole (71.53%) at 1 mmol/L concentration. Compounds **3a–e, 3g** and **3h** showed promising *in vivo* anti-inflammatory activity (ranging from 62.25% to 80.93%) in comparison to diclofenac sodium (81.62%). The ulcerogenic liability and lipid peroxidation activity of these compounds were observed to be less in comparison to diclofenac sodium. These compounds also potently inhibited the lipopolysaccharide (LPS)-induced TNF-α release in mice (ID_{50} of **3a–c** = 19.98, 11.32 and 9.67 mg/kg, respectively). Among the screened compounds, derivative **3c** was found to be the most potent and its binding mode within the p38α MAPK is also reported.

*Corresponding author. Tel.:+91 9013476217.
E-mail address: mamir_s2003@yahoo.co.in (Mohammad Amir).

Peer review under responsibility of Institute of Materia Medica, Chinese Academy of Medical Sciences and Chinese Pharmaceutical Association.

http://dx.doi.org/10.1016/j.apsb.2016.08.006

1. Introduction

Inflammation is a multifactorial, protective attempt of the non-specific immune system. In response to infection stimulus, monocytes/macrophages lineage cells are activated, thereby generating an inflammatory environment by secreting proinflammatory cytokines. It is an important aspect in rheumatoid arthritis, osteoarthritis, Alzheimer's disease and obesity related diseases[1]. Non-steroidal anti-inflammatory drugs (NSAIDs) are amongst the most widely prescribed agents for the management of various inflammatory diseases[2,3]. NSAIDs act by counteracting the cyclooxygenase (COX) that converts arachidonic acid into prostaglandins in inflammatory processes. Commonly used NSAIDs, such as aspirin, indomethacin and diclofenac, are non-selective inhibitors and are responsible for adverse side effects, such as gastric ulceration, bleeding and renal function suppression[4]. There are at least two mammalian COX isoforms[5,6]. COX-1 is constitutive and provides cytoprotection in the gastrointestinal (GI) tract, while COX-2 is induced and responsible for pro-inflammatory conditions[4]. Various selective COX-2 inhibitors, such as celecoxib, rofecoxib and valdecoxib, showed anti-inflammatory activity with minimum gastric side effects[7]. Unfortunately, selective COX-2 inhibitors were found to cause cardiovascular side effects[8]. Therefore, in view of the GI toxicity of conventional NSAIDs and the adverse cardiovascular side effects of selective COX-2 inhibitors, there is a need to develop anti-inflammatory agents with an improved safety profile.

p38α mitogen activated protein kinase (MAPK) has attracted considerable attention as a major target in developing anti-inflammatory drugs. Activated p38α phosphorylates a range of intracellular protein substrates that transcriptionally regulate the biosynthesis of inflammatory cytokines like tumor necrosis factor-α (TNF-α) and interleukin-1β (IL-1β)[9]. The identification of p38 MAPK as the target of some pyridinyl-imidazole compounds, *e.g.* SB203580 (Fig. 1A), confirmed the role of this intracellular enzyme in the regulation of many physiological and pathological states and reinforced the importance of its modulation in the therapy of many inflammatory diseases[10]. p38α MAPK belongs to the serine/threonine family of kinases and is a key enzyme of a cascade leading to the production of pro-inflammatory cytokines, such as IL-1β and TNF-α[11]. Excessive levels of these cytokines are known to be involved in the progression of many inflammatory disorders, such as rheumatoid arthritis, inflammatory bowel disease, and psoriasis[12–14]. TNF-α is a major pleiotropic pro-inflammatory cytokine and is known to activate platelets and also participates in the genesis of fever and anemia[15]. Increased production of TNF-α also modulates processes, such as immune cell activation, proliferation, apoptosis and leukocyte migration and is thereby associated with many inflammatory diseases, like Crohn's disease, psoriasis, multiple sclerosis and rheumatoid arthritis[16]. p38α MAPK inhibition is therefore a promising therapeutic strategy to block the biosynthesis of TNF-α.

Pyrazole derivatives are an important class of heterocycles because of their diverse pharmacological properties, such as antioxidant, anti-inflammatory, antimicrobial and anti-viral/anti-tumor effects. Rofecoxib and celecoxib (selective COX-2 inhibitors) having a pyrazole moiety have exhibited significant anti-inflammatory activity with reduced GI toxicity. Furthermore, pyrazoles[17] and pyrazolyl urea derivatives have also been reported to be potential anti-inflammatory agents[18–20]. Compound BIRB-796[20] (Fig. 1B) having pyrazolyl urea moiety has shown significant anti-inflammatory activity through p38α MAPK and TNF-α inhibition and had advanced into clinical trials.

Encouraged by these observations and in the course of our research program on the synthesis of five membered heterocyclic compounds as anti-inflammatory agents[10,21–24], we report herein the synthesis and evaluation of some new pyrazolyl urea derivatives as potential anti-inflammatory agents.

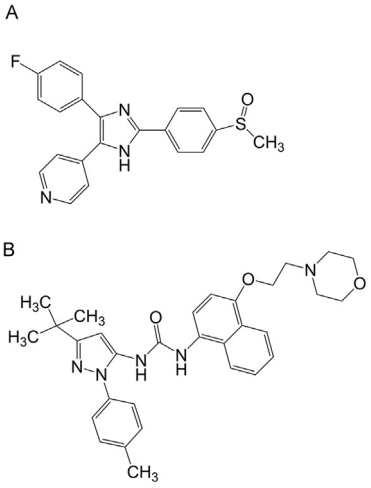

Figure 1 Compound structures of (A) SB 203580 and (B) BIRB 796 (Doramapimod).

2. Results and discussion

2.1. Chemistry

The titled compounds **3a–o** were synthesized as illustrated in Scheme 1. The pyrazoles **1a–o** were synthesized as reported earlier[25]. Compounds **1a–o** were then treated with 4-nitrophenylchloroformate in acetonitrile in the presence of pyridine to afford phenylcarbamate derivatives **2a–o**. The pyrazolyl urea derivatives **3a–o** were synthesized by treating compounds **2a–o** with ammonium acetate in THF in the presence of triethylamine. Many literature revealed the use of benzylisocyanate for converting amino groups into ureas. In the present study, benzylisocyanate was used for the preparation of urea derivatives but the reaction failed to yield the desired products. Further literature surveys revealed that amines when treated with 4-nitrophenylchloroformate, followed by the treatment with ammonium acetate, provided the corresponding ureas in high yield and purity even in aqueous environment. Following this method the titled compounds were obtained in good yields and were found to be pure.

The NH_2 protons of the pyrazoles **1a–o** were observed at δ 5.17–5.24, which disappeared in the phenyl carbamate derivatives **2a–o**. Appearance of a singlet for CONH protons from δ 10.21–10.47 confirmed the formation of phenyl carbamate derivatives. The formation of **3a–o** was confirmed by the appearance of a singlet for NH_2 protons from δ 6.12–6.23 showing the presence of a urea group in the compounds. Compounds **3a–o** also showed a singlet for the CONH protons from δ 10.13 to 10.55. The ^{13}C NMR spectral data of **3a–o** showed characteristic peaks for C=O carbons from δ 170.11 to 171.96. The pyrazole carbons were detected at δ 159.21 to 161.48 (pyrazole C_3), δ 102.48 to 105.68 (pyrazole C_4) and δ 150.97 to 159.66 (pyrazole C_5). The OCH_2 carbon showed distinct peaks at δ 70.19 to 72.54. Mass spectra of compounds **3a–o** showed molecular ion peaks M^+ at an *m/z* corresponding to their molecular formula.

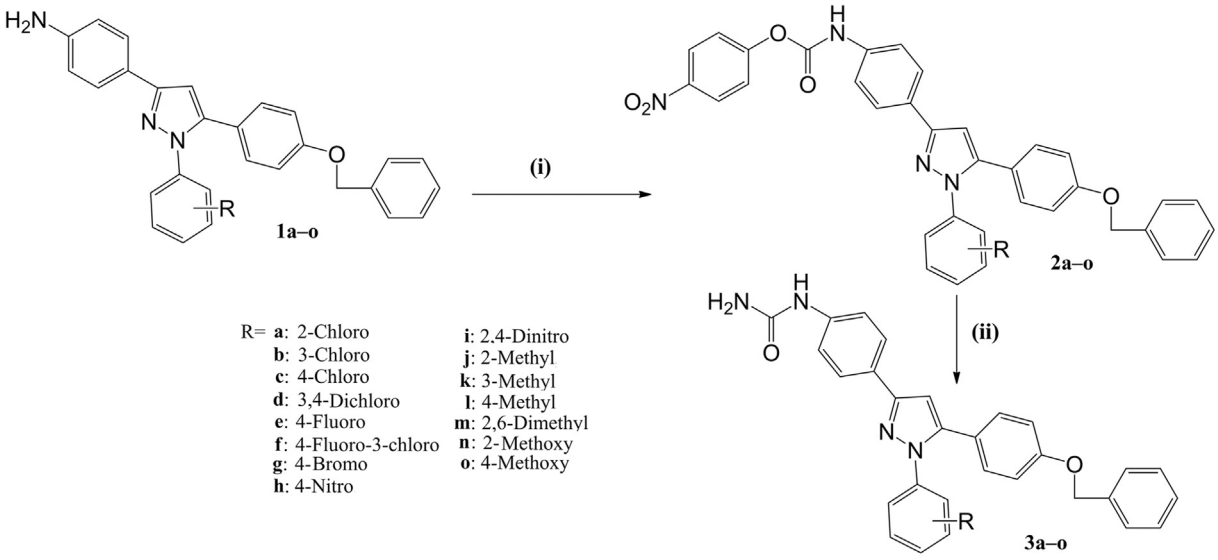

Scheme 1 Reaction protocol for the synthesis of **3a–o**. Reagent and conditions: **(i)** 4-nitrophenylchloroformate, pyridine, CH_3CN; **(ii)** ammonium acetate, Et_3N, THF.

2.2. *p38α MAPK assay*

The modulation of p38α MAPK activity by all the synthesized compounds **3a–o** was determined in an enzyme assay measuring the inhibition of the p38α MAPK mediated ATF-2 phosphorylation. Compound **3c** with a 4-chlorophenyl group at position 1 of the pyrazole ring exhibited the strongest p38α MAPK inhibition (IC_{50} = 0.037 ± 1.56 µmol/L) in comparison to the reference standard, SB 203580 (IC_{50} = 0.043 ± 3.62 µmol/L). Substitution of the 4-chlorophenyl group by 2-chloro (**3a**), 3-chloro (**3b**), 4-fluoro (**3e**) and 4-bromo (**3g**) groups also led to similar p38α MAPK activity (IC_{50} = 0.039 ± 0.04, 0.039 ± 1.50, 0.048 ± 0.01, 0.042 ± 1.22 µmol/L, respectively). The IC_{50} value was decreased slightly for compound **3h** having a 4-nitro group (IC_{50} = 0.067 ± 0.95 µmol/L). Replacement with a disubstituted electron withdrawing groups, such as 3,4-dichloro (**3d**), 2,4-dinitro (**3i**) and 4-fluoro-3-chloro (**3f**), resulted in further decrease of p38α MAPK inhibitory activity (IC_{50} = 0.079 ± 0.65, 0.112 ± 0.04 and 0.110 ± 0.17 µmol/L, respectively). When electron withdrawing groups were replaced with electron donating groups like 2-methyl (**3j**), 3-methyl (**3k**), 4-methyl (**3l**), 2-methoxy (**3n**) and 4-methoxy (**3o**), led to a further decrease of activity (IC_{50} ranging from 0.123 ± 1.74 to 0.210 ± 0.11 µmol/L). It was observed that when these electron donating groups were replaced by disubstituted methyl group (2,6-dimethyl, **3m**), the activity was found to be minimum (IC_{50} = 0.270 ± 4.22 µmol/L) (Table 1). Thus the initial activity profile suggests that electron withdrawing groups attached to the position 1 of pyrazole ring were more active than electron donating groups. Furthermore, monosubstituted compounds were found to be more active than disubstituted compounds. On the basis of these results, seven compounds (**3a–e**, **3g** and **3h**) showing good inhibitory activity were selected for the *in vivo* anti-inflammatory activity screening.

Table 1 IC_{50} values against p38α MAPK and XP docking glide score of **3a–o** and the standard, SB 203580.

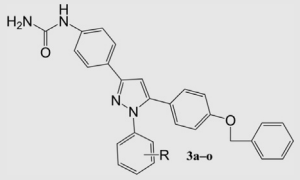

Compd.	R	IC_{50} value (µmol/L)[a]	Glide score[b]
3a	2-Cl	0.039±0.04	−8.197
3b	3-Cl	0.039±1.50	−8.782
3c	4-Cl	0.037±1.56	−8.872
3d	3,4-diCl	0.079±0.65	−8.083
3e	4-F	0.048±0.01	−8.705
3f	4-F-3-Cl	0.110±0.17	−9.175
3g	4-Br	0.042±1.22	−8.818
3h	4-NO_2	0.067±0.95	−7.610
3i	2,4-diNO_2	0.112 ±0.04	−7.159
3j	2-CH_3	0.123±1.74	−8.227
3k	3-CH_3	0.210±0.11	−8.520
3l	4-CH_3	0.169±0.07	−8.945
3m	2,6-diCH_3	0.270±4.22	−7.567
3n	2-OCH_3	0.206±0.37	−8.012
3o	4-OCH_3	0.170±0.87	−7.753
SB 203580	–	0.043±3.62	−8.795

[a]Mean ± SEM of three experiments.
[b]Glide score denotes *g* score obtained for docking with p38α MAPK (PDB ID: 3D83).

2.3. *Antioxidant activity*

In this study all the synthesized compounds were evaluated for their free radical scavenging property by measuring the decrease in the absorption of the stable 2,2′-diphenyl-1-picryl hydrazyl radical (DPPH) at 517 nm. This bleaching occurs when the odd electron of the radical is paired and is independent of any enzymatic activity. All the tested compounds showed antioxidant activity ranging from 75.06% to 31.75% when compared to a standard butylated hydroxy anisole (BHA) (71.53%). The most active compound of the series was found to be **3c** showing 75.06% antioxidant activity. Unfortunately compounds **3j**, **3n** and **3o** did not exhibit any significant antioxidant activity (Fig. 2).

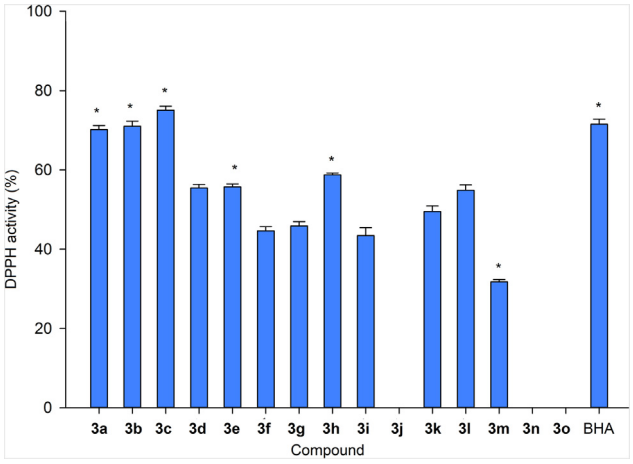

Figure 2 Antioxidant activity of derivatives **3a–o.** Compounds **3j**, **3n** and **3o** did not exhibit significant antioxidant activity. Data are expressed as mean ± SD, $n=3$. *$P<0.05$ compared to BHA. BHA: butylated hydroxy anisole.

2.4. *Anti-inflammatory activity*

Compounds **3a–e**, **3g** and **3h** showing good p38α MAPK inhibitory activity (IC_{50} ranging from 0.037 ± 1.56 to 0.079 ± 0.65 µmol/L) were further evaluated for their anti-inflammatory activity (*in vivo*) by the carrageenan-induced rat paw edema method. The compounds and standard drug, diclofenac sodium, were tested at an equimolar oral dose (10 mg/kg body weight). The tested compounds showed anti-inflammatory activity ranging from 62.25% to 80.93%, whereas the standard drug showed 81.72% inhibition after 4h. It was observed that compound **3c** having a 4-chloro group showing high p38α MAPK activity also showed the highest anti-inflammatory activity (80.93% inhibition). Replacement of 4-chloro group by 2-chloro (**3a)** and 3-chloro (**3b**) groups resulted in a slight decrease of activity (76.19% and 78.06% inhibition, respectively). Substitution with a 4-fluoro (**3e**), 4-bromo (**3g**) and 4-nitro (**3h**) groups resulted in further decrease of anti-inflammatory activity (72.33%, 74.01% and 68.38% inhibition, respectively). Compound **3d** having a disubstituted group (3,4-dichloro) showed minimum anti-inflammatory activity (62.25% inhibition, Table 2). It was observed that monosubstituted electron withdrawing groups in the phenyl ring attached to the pyrazole nucleus showed good anti-inflammatory activity in both the *in vitro* and *in vivo* models.

Table 2 Anti-inflammatory activity of **3a–e**, **3g**, **3h** and diclofenac sodium.

Compd.	Increase in paw edema (mL)[a]	Inhibition (%)	Activity relative to diclofenac sodium
3a	0.40±0.08	76.19[b]	93.23
3b	0.37±0.20	78.06[b]	95.52
3c	0.32±0.06	80.93[b]	99.03
3d	0.64±0.05	62.25	76.17
3e	0.47±0.16	72.33	88.50
3g	0.44±0.06	74.01[b]	90.56
3h	0.53±0.12	68.38	83.67
Control	1.69±0.04	–	–
Diclofenac sodium	0.31±0.13	81.72	100

– not applicable.
[a]Data are expressed as mean±SEM, and analyzed by Student's *t*-test for $n=6$.
[b]Values are statistically significant compared to control group ($P<0.05$).

2.5. *Ulcerogenic potential and lipid peroxidation*

Compounds **3a–e, 3g** and **3h** were also tested for their ulcerogenic activity at an oral dose of 30 mg/kg. Compound **3c** showed minimum ulcerogenicity (severity index 0.58 ± 0.37). Compounds **3a**, **3b**, **3d, 3e, 3g** and **3h** also showed reduction in severity index (ranging from 0.67 ± 0.25 to 1.08 ± 0.37) superior to the standard drug, diclofenac (severity index 1.83 ± 0.27) (Table 3). Thus it was observed that the tested compounds have better GI safety profile than the standard drug.

The compounds showing high anti-inflammatory activity and reduced ulcerogenic potential were also tested for their lipid peroxidation, which was measured as nmol of malondialdehyde (MDA) per 100 mg of gastric mucosal tissue. The control group showed 3.26 ± 0.12 nmol/100 mg of lipid peroxidation, whereas diclofenac sodium (standard drug) showed 6.52 ± 0.42 nmol/100 mg MDA. It was found that all the tested compounds showed reduced lipid peroxidation superior to the standard drug except compounds **3d** and **3h,** which showed slightly higher lipid peroxidation (Table 3). Thus it may be concluded that the protection of gastric mucosa might be related to the inhibition of lipid peroxidation.

2.6. *TNF-α production inhibition evaluation*

Compounds **3a–e**, **3g** and **3h** were also evaluated for their inhibitory activity against lipopolysaccharide (LPS)-induced

Table 3 Ulcerogenic, lipid peroxidation and TNF-α inhibition activities of **3a–e**, **3g**, **3h** and the standards.

Compd.	Severity index[a]	Lipid peroxidation (nmol MDA/100 mg tissue)[a]	TNF-α inhibition (%)[a]	ID_{50} (mg/kg)
Control	0.00±0.00	3.26±0.12	–	–
3a	0.67±0.25[b]	5.47±0.44[b]	60.87±2.65[b]	19.98
3b	0.67±0.40[b]	5.19±0.48[b]	62.45±0.07[b]	11.32[b]
3c	0.58±0.37[b]	5.12±0.55[b]	62.56±0.24	9.67[b]
3d	1.08±0.37[b]	6.83±0.48[b]	52.60±2.16	–
3e	0.83±0.22	6.08±0.15	57.34±3.05	–
3g	0.75±0.27	6.02±0.17[a]	58.13±0.28	–
3h	0.91±0.20	6.84±0.18	52.76±2.08	–
Diclofenac sodium	1.83±0.27	6.52±0.42	–	–
SB 203580	–	–	52.11±1.08[b]	28.40[b]

– not applicable.
[a]Data were expressed as mean±SEM and analyzed by Student's *t*-test for $n=6$.
[b]Values are statistically significant compared to respective standard ($P<0.05$).

TNF-α production in mice. Compound **3c** was found to be most effective with an ID_{50} value of 9.67 mg/kg, which was more active than that of SB 203580 (ID_{50} = 28.40 mg/kg). Analogs **3a** and **3b** also demonstrated good TNF-α inhibitory efficacy with ID_{50} values of 19.98 and 11.32 mg/kg, respectively (Table 3).

2.7. *Docking study*

The crystal structures of p38α MAPK complexed with inhibitors were selected as the protein target used for the docking study. Among the compounds studied for p38α MAPK inhibition, compound **3c** showing high p38α MAPK activity (IC_{50}= 0.037 $\pm$ 1.56 µmol/L) and *in vivo* anti-inflammatory activity (80.93% inhibition) was found to be potent. The most stable docking pose was selected according to the best docking scored conformation predicted by the Glide scoring function. The orientation and conformation of the docked compound are similar to those of SB 203580 (p38α prototype inhibitor). The binding modes of **3c** and the prototype inhibitor (SB 203580) to a rearranged (DFG-out) form of p38α are presented in Fig. 3. Compound **3c** and SB 203580 showed a common interaction with amino acid residue ASP 168 and LYS 53. The nitrogen atom of pyrazole scaffold of **3c** formed hydrogen bond with the backbone of ASP 168 (N…. HN, 2.65 Å). The oxygen atom in the carbonyl functionality in **3c** forms a hydrogen bond with the side chain of LYS 53 (C=O…. HN, 3.84 Å) residue in the binding pocket, shown in Fig. 3A. Moreover the urea moiety forms additional hydrogen bonds with THR 106 (H….OH, 2.14 Å) and Ala 51 (O….HN, 2.25 Å; O…. HN, 3.73 Å). The receptor surface view of compound **3c** in the protein is shown in Fig. 3B and superimposed docked pose of compound **3c** with SB 203580 is also represented in Fig. 3D, which confirms their identical orientation and alignment. Furthermore, the docked pose of SB 203580 revealed that the pyrazole NH and N atoms formed two hydrogen bonds with the side chain of GLU 71 (1.89 Å, H…O) and backbone of ASP 168 (2.70 Å, N…H) in the binding pocket. Finally, SB 203580 adopts a favorable conformation in which one of the phenyl ring formed a π-cation interaction with LYS 53 (4.21 Å, Phenyl…$^{+}$HN). The glide scores of **3a–o** were in the range of −9.175 to −7.159. Compound **3c** showed a glide score of −8.872 and SB 203580 had a glide score of −8.795 (Table 1).

3. Conclusions

Fifteen new pyrazolyl urea derivatives have been synthesized and subjected to *in vitro* screening for p38α MAPK inhibition and antioxidant activities. Moreover, the *in vivo* anti-inflammatory, ulcerogenic, lipid peroxidation and TNF-α inhibition activities of the compounds have also been tested. The results of the *in vitro* activities revealed that compounds **3a–e**, **3g** and **3h** bearing 2-chloro, 3-chloro, 4-chloro, 3,4-dichloro, 4-fluoro, 4-bromo and 4-nitro phenyl groups, respectively, at the position 1 of pyrazole ring showed better p38α MAPK inhibition as compared to the standard inhibitor (SB 203580). Compound **3c** was found to have superior antioxidant activity in comparison to the reference compound, BHA. It was noted that compound **3c** was a potent anti-inflammatory agent comparable to the standard reference drug diclofenac sodium. This compound also showed reduced ulcerogenic potential and the weakest activity in inducing oxidative

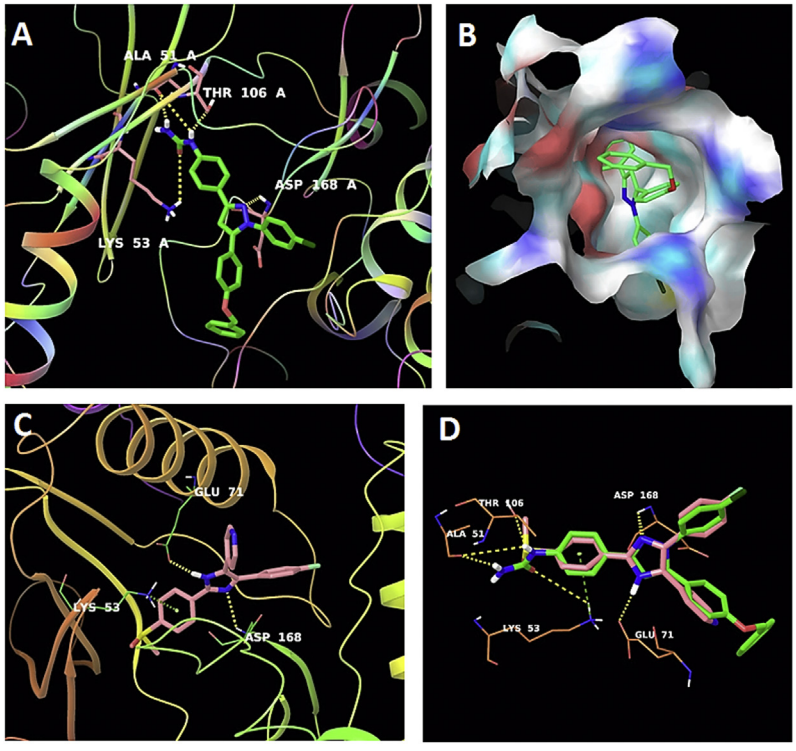

Figure 3 (A) Docked pose of compound **3c** (green color) represented as tube in the binding site of p38α MAPK showing hydrogen bond interaction (yellow dashed lines) with ASP 168, LYS 53, ALA 51 and THR 106; (B) Receptor surface view of compound **3c** (green color) (C) Docked pose of SB 203580 (pink color) represented as tube in the binding site of p38α MAPK showing hydrogen bond interaction (yellow dashed lines) with ASP 168, GLU 71 and π-cation interaction with LYS 53; (D) Superimposed docked pose of compound **3c** (green color) with SB 203580 (pink color) in the binding site.

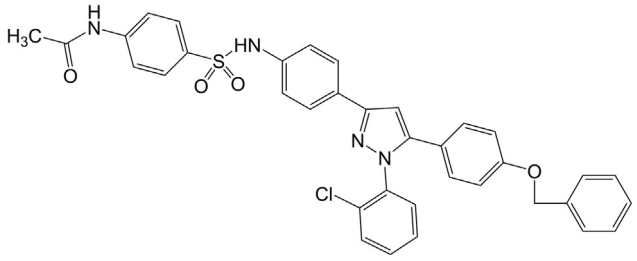

Figure 4 Structure of compound **4a**

stress in tissues compared to the standard drug. Compound **3c** also demonstrated good inhibition of LPS-induced TNF-α production in mice. It was observed that compounds showing significant *in vitro* p38α MAPK activity also showed good *in vivo* anti-inflammatory and TNF-α inhibitory activities. In summary, among all the tested compounds, 1-[4-[5-(4-(benzyloxy)phenyl)-1-(4-chlorophenyl)-1*H*-pyrazol-3-yl]phenyl]urea (**3c**) was the most potent anti-inflammatory agent having reduced ulcerogenic liability and lipid peroxidation.

Our earlier studies on pyrazole derivatives having a sulfonamide moiety[24] also showed good anti-inflammatory and TNF-α inhibitory activities. Compound **4a** (Fig. 4) having 2-chloro group at the position 1 of pyrazole ring has shown high anti-inflammatory and TNF-α inhibitory activities. Whereas in the present studies, pyrazole derivatives having a urea pharmacophore also showed comparable anti-inflammatory activity along with improved TNF-α inhibitory properties. Furthermore, pyrazolyl urea derivatives were also studied for their p38α MAPK inhibition and showed significant activity.

4. Experimental

4.1. Chemistry

Melting points (mp, °C) were recorded using a Labtronics digital melting point apparatus (Haryana, India) and were uncorrected. IR spectra were recorded on a Perkin-Elmer 1720 FTIR spectrometer (New York, USA). ^{1}H NMR spectra (400 MHz) and ^{13}C NMR spectra (100 MHz) were obtained on a Bruker Avance NMR spectrometer (Zurich, Switzerland) using tetramethysilane (TMS) as the internal reference with complete proton decoupling. MS analyses were performed on a Jeol SX-102 spectrometer (Tokyo, Japan). Thin layer chromatography (TLC) was performed on silica gel G (Merck) and spots were visualized under the ultraviolet light (UV 254 nm). Elemental analyses (C, H and N) were conducted using a CHNS Vario EL III machine (Elementar Analysen systeme GmbH, Germany).

*4.1.1. 4-[5-[4-(Benzyloxy)phenyl]-1-substituted phenyl-1H-pyrazol-3-yl]anilines (**1a–o**)*

The compounds were synthesized using our earlier reported method[24].

*4.1.2. General method for the synthesis of 4-nitrophenyl 4-[5-(4-(benzyloxy)phenyl)-1-substituted-1H-pyrazol-3-yl] phenylcarbamates (**2a–o**)*

A mixture of one equivalent of the 4-[5-(4-(benzyloxy)phenyl)-1-substituted phenyl-1*H*-pyrazol-3-yl]anilines **1a–o** (5 mmol), five equivalents of 4-nitrophenylchloroformate (25 mmol) and 5 equivalents of pyridine (5 mL) in the presence of acetonitrile (20 mL) was stirred at room temperature for 3–5 h. The reaction mixture was quenched with water (100 mL). An oily material thus obtained was kept aside overnight at room temperature. Solid thus obtained was filtered, washed with water, dried and recrystallized from ethanol.

*4.1.2.1. 4-Nitrophenyl-4-[5-(4-(benzyloxy)phenyl)-1-(2-chlorophenyl)-1H-pyrazol-3-yl]phenyl carbamate (**2a**).* Yield 82%; mp 157–158 °C; IR (cm^{-1}, KBr): 3031 (C-H), 1670 (CONH), 1598 (C=N); ^{1}H NMR (DMSO-d_6): δ 10.27 (s, 1H, CONH, D_2O exchangeable), 7.42–7.89 (m, 21H, Ar-H), 7.05 (s, 1H, pyrazole-H-4), 5.12 (s, 2H, OCH_2); Anal. Calcd. for $C_{35}H_{25}ClN_4O_5$: C, 68.13; H, 4.08; N, 9.08; Found: C, 68.20; H, 4.02; N, 9.11.

*4.1.2.2. 4-Nitrophenyl-4-[5-(4-(benzyloxy)phenyl)-1-(3-chlorophenyl)-1H-pyrazol-3-yl]phenyl carbamate (**2b**).* Yield 84%; mp 154–156 °C; IR (cm^{-1}, KBr): 3031 (C–H), 1666 (C=O), 1592 (C=N); ^{1}H NMR (DMSO-d_6): δ 10.25 (s, 1H, CONH, D_2O exchangeable), 7.47–7.88 (m, 21H, Ar–H), 7.02 (s, 1H, pyrazole-H-4), 5.16 (s, 2H, OCH_2); Anal. Calcd. for $C_{35}H_{25}ClN_4O_5$: C, 68.13; H, 4.08; N, 9.08; Found: C, 68.23; H, 4.14; N, 9.07.

*4.1.2.3. 4-Nitrophenyl-4-[5-(4-(benzyloxy)phenyl)-1-(4-chlorophenyl)-1H-pyrazol-3-yl]phenyl carbamate (**2c**).* Yield 79%; mp 163–164 °C; IR (cm^{-1}, KBr): 3035 (C-H), 1668 (CONH), 1595 (C=N); ^{1}H NMR (DMSO-d_6): δ 10.36 (s, 1H, CONH, D_2O exchangeable), 7.43–7.89 (m, 21H, Ar-H), 7.09 (s, 1H, pyrazole-H-4), 5.21 (s, 2H, OCH_2); Anal. Calcd. for $C_{35}H_{25}ClN_4O_5$: C, 68.13; H, 4.08; N, 9.08; Found: C, 68.06; H, 4.03; N, 9.05.

*4.1.2.4. 4-Nitrophenyl-4-[5-(4-(benzyloxy)phenyl)-1-(3,4-dichlorophenyl)-1H-pyrazol-3-yl]phenyl carbamate (**2d**).* Yield 77%; mp 158–159 °C; IR (cm^{-1}, KBr): 3031 (C-H), 1672 (CONH), 1596 (C=N); ^{1}H NMR (DMSO-d_6): δ 10.47 (s, 1H, CONH, D_2O exchangeable), 7.42–7.91 (m, 20H, Ar-H), 7.11 (s, 1H, pyrazole-H-4), 5.13 (s, 2H, OCH_2); Anal. Calcd. for $C_{35}H_{24}Cl_2N_4O_5$: C, 64.52; H, 3.71; N, 8.60; Found: C, 64.56; H, 3.64; N, 8.65.

*4.1.2.5. 4-Nitrophenyl-4-[5-(4-(benzyloxy)phenyl)-1-(4-fluorophenyl)-1H-pyrazol-3-yl]phenyl carbamate (**2e**).* Yield 82%; mp 186–187 °C; IR (cm^{-1}, KBr): 3032 (C-H), 1663 (CONH), 1585 (C=N); ^{1}H NMR (DMSO-d_6): δ 10.44 (s, 1H, CONH, D_2O exchangeable), 7.39–7.88 (m, 21H, Ar-H), 7.05 (s, 1H, pyrazole-H-4), 5.18 (s, 2H, OCH_2); Anal. Calcd. for $C_{35}H_{25}FN_4O_5$: C, 69.99; H, 4.20; N, 9.33; Found: C, 69.96; H, 4.13; N, 9.27.

*4.1.2.6. 4-Nitrophenyl-4-[5-(4-(benzyloxy)phenyl)-1-(4-fluoro-3-chlorophenyl)-1H-pyrazol-3-yl]phenyl carbamate (**2f**).* Yield 75%; mp 202–203 °C; IR (cm^{-1}, KBr): 3033 (C-H), 1672 (CONH), 1590 (C=N); ^{1}H NMR (DMSO-d_6): δ 10.21 (s, 1H, CONH, D_2O exchangeable), 7.42–7.85 (m, 20H, Ar-H), 7.08 (s, 1H, pyrazole-H-4), 5.16 (s, 2H, OCH_2); Anal. Calcd. for $C_{35}H_{24}ClFN_4O_5$: C, 66.20; H, 3.81; N, 8.82; Found: C, 66.16; H, 3.83; N, 8.75.

*4.1.2.7. 4-Nitrophenyl-4-[5-(4-(benzyloxy)phenyl)-1-(4-bromophenyl)-1H-pyrazol-3-yl]phenyl carbamate (**2g**).* Yield 77%; mp 171–172 °C; IR (cm^{-1}, KBr): 3031 (C-H), 1658 (CONH), 1590 (C=N); ^{1}H NMR (DMSO-d_6): δ 10.26 (s, 1H, CONH, D_2O exchangeable), 7.40–7.84 (m, 21H, Ar-H), 7.05 (s, 1H, pyrazole-H-4), 5.16 (s, 2H, OCH_2); Anal. Calcd. for $C_{35}H_{25}BrN_4O_5$: C, 63.55; H, 3.81; N, 8.47; Found: C, 63.61; H, 3.89; N, 8.45.

*4.1.2.8. 4-Nitrophenyl-4-[5-(4-(benzyloxy)phenyl)-1-(4-nitrophenyl)-1H-pyrazol-3-yl]phenyl carbamate (**2h**).* Yield 81%; mp

188–189 °C; IR (cm^{-1}, KBr): 3030 (C-H), 1671 (CONH), 1594 (C=N); ^{1}H NMR (DMSO-d_6): δ 10.33 (s, 1H, CONH, D_2O exchangeable), 7.36–7.82 (m, 21H, Ar-H), 7.07 (s, 1H, pyrazole-H-4), 5.09 (s, 2H, OCH_2); Anal. Calcd. for $C_{35}H_{25}N_5O_7$: C, 66.98; H, 4.02; N, 11.16; Found: C, 66.96; H, 4.09; N, 11.09.

*4.1.2.9. 4-Nitrophenyl-4-[5-(4-(benzyloxy)phenyl)-1-(2,4-dinitrophenyl)-1H-pyrazol-3-yl]phenyl carbamate (**2i**).* Yield 89%; mp 178–179 °C; IR (cm^{-1}, KBr): 3031 (C-H), 1673 (C=O), 1597 (C=N); ^{1}H NMR (DMSO-d_6): δ 10.39 (s, 1H, CONH, D_2O exchangeable), 7.42–7.86 (m, 20H, Ar-H), 7.05 (s, 1H, pyrazole-H-4), 5.16 (s, 2H, OCH_2); Anal. Calcd. for $C_{35}H_{24}N_6O_9$: C, 62.50; H, 3.60; N, 12.49; Found: C, 62.56; H, 3.68; N, 12.54.

*4.1.2.10. 4-Nitrophenyl 4-[5-(4-(benzyloxy)phenyl)-1-(2-methylphenyl)-1H-pyrazol-3-yl]phenyl carbamate (**2j**).* Yield 81%; mp 181–183 °C; IR (cm^{-1}, KBr): 3029 (C-H), 1656 (CONH), 1588 (C=N); ^{1}H NMR (DMSO-d_6): δ 10.29 (s, 1H, CONH, D_2O exchangeable), 7.42–7.84 (m, 21H, Ar-H), 7.05 (s, 1H, pyrazole-H-4), 5.10 (s, 2H, OCH_2), 2.27 (s, 3H, CH_3); Anal. Calcd. for $C_{36}H_{28}N_4O_5$: C, 72.47; H, 4.73; N, 9.39; Found: C, 72.52; H, 4.79; N, 9.31.

*4.1.2.11. 4-Nitrophenyl 4-[5-(4-(benzyloxy)phenyl)-1-(3-methylphenyl)-1H-pyrazol-3-yl]phenyl carbamate (**2k**).* Yield 84%; mp 184–185 °C; IR (cm^{-1}, KBr): 3037 (C-H), 1674 (CONH), 1592 (C=N); ^{1}H NMR (DMSO-d_6): δ 10.34 (s, 1H, CONH, D_2O exchangeable), 7.41–7.87 (m, 21H, Ar-H), 7.05 (s, 1H, pyrazole-H-4), 5.11 (s, 2H, OCH_2), 2.29 (s, 3H, CH_3); Anal. Calcd. for $C_{36}H_{28}N_4O_5$: C, 72.47; H, 4.73; N, 9.39; Found: C, 72.48; H, 4.76; N, 9.35.

*4.1.2.12. 4-Nitrophenyl 4-[5-(4-(benzyloxy)phenyl)-1-(4-methylphenyl)-1H-pyrazol-3-yl]phenyl carbamate (**2l**).* Yield 81%; mp 185–186 °C; IR (cm^{-1}, KBr): 3031 (C-H), 1663 (CONH), 1585 (C=N); ^{1}H NMR (DMSO-d_6): δ 10.38 (s, 1H, CONH, D_2O exchangeable), 7.36–7.93 (m, 21H, Ar-H), 7.05 (s, 1H, pyrazole-H-4), 5.22 (s, 2H, OCH_2), 2.30 (s, 3H, CH_3); Anal. Calcd. for $C_{36}H_{28}N_4O_5$: C, 72.47; H, 4.73; N, 9.39; Found: C, 72.53; H, 4.68; N, 9.34.

*4.1.2.13. 4-Nitrophenyl-4-[5-(4-(benzyloxy)phenyl)-1-(2,6-dimethylphenyl)-1H-pyrazol-3-yl]phenyl carbamate (**2m**).* Yield 74%; mp 193–195 °C; IR (cm^{-1}, KBr): 3037 (C-H), 1668 (CONH), 1592 (C=N); ^{1}H NMR (DMSO-d_6): δ 10.23 (s, 1H, CONH, D_2O exchangeable), 7.42–7.82 (m, 20H, Ar-H), 7.05 (s, 1H, pyrazole-H-4), 5.12 (s, 2H, OCH_2), 2.17 (s, 6H, CH_3); Anal. Calcd. for $C_{37}H_{30}N_4O_5$: C, 72.77; H, 4.95; N, 9.17; Found: C, 72.73; H, 4.98; N, 9.24.

*4.1.2.14. 4-Nitrophenyl-4-[5-(4-(benzyloxy)phenyl)-1-(2-methoxyphenyl)-1H-pyrazol-3-yl]phenyl carbamate (**2n**).* Yield 72%; mp 165–166 °C; IR (cm^{-1}, KBr): 3029 (C–H), 1661 (CONH), 1595 (C=N); ^{1}H NMR (DMSO-d_6): δ 10.35 (s, 1H, CONH, D_2O exchangeable), 7.42–7.88 (m, 21H, Ar-H), 7.05 (s, 1H, pyrazole-H-4), 5.18 (s, 2H, OCH_2), 3.69 (s, 3H, OCH_3); Anal. Calcd. for $C_{36}H_{28}N_4O_6$: C, 70.58; H, 4.61; N, 9.15; Found: C, 70.53; H, 4.68; N, 9.09.

*4.1.2.15. 4-Nitrophenyl-4-[5-(4-(benzyloxy)phenyl)-1-(4-methoxyphenyl)-1H-pyrazol-3-yl]phenyl carbamate (**2o**).* Yield 77%; mp 169–170 °C; IR (cm^{-1}, KBr): 3032 (C-H), 1674 (CONH), 1590 (C=N); ^{1}H NMR (DMSO-d_6): δ 10.41 (s, 1H, CONH, D_2O exchangeable), 7.38–7.92 (m, 21H, Ar-H), 7.03 (s, 1H, pyrazole-H-4), 5.21 (s, 2H, OCH_2), 3.72 (s, 3H, OCH_3); Anal. Calcd. for $C_{36}H_{28}N_4O_6$: C, 70.58; H, 4.61; N, 9.15; Found: C, 70.51; H, 4.57; N, 9.11.

*4.1.3. General method for the synthesis of 1-[4-[5-(4-(benzyloxy)phenyl)-1-(substituted phenyl)-1H-pyrazol-3-yl]phenyl] ureas (**3a–o**)*

A mixture of 4-nitrophenyl-4-[5-(4-(benzyloxy)phenyl)-1-substituted-1*H*-pyrazol-3-yl]phenyl carbamates **2a–o** (5 mmol) and ammonium acetate (20 mmol) in the presence of triethylamine (20 mmol) and tetrahydrofuran (20 mL) was stirred at room temperature for 4–6 h. The reaction mixture was then poured into ice water (30 mL) while stirring. The compound obtained was filtered, washed with water and dried. The residue thus obtained was triturated in hot DCM, filtered and recrystallized from ethanol.

*4.1.3.1. 1-[4-[5-(4-(Benzyloxy)phenyl)-1-(2-chlorophenyl)-1H-pyrazol-3-yl]phenyl]urea (**3a**).* Yield 64%; mp 210–211 °C; IR (cm^{-1}, KBr): 3352 (N-H), 3031 (C-H), 1652 (CONH), 1598 (C=N); ^{1}H NMR (DMSO-d_6): δ 10.32 (s, 1H, CONH, D_2O exchangeable), 7.49–8.16 (m, 17H, Ar-H), 7.12 (s, 1H, pyrazole-H-4), 6.18 (s, 2H, NH_2, D_2O exchangeable), 5.23 (s, 2H, OCH_2); ^{13}C NMR (DMSO-d_6): δ 170.17 (C=O), 161.25 (pyrazole C_3), 150.97 (pyrazole C_5), 144.74, 138.25, 135.11, 135.07, 134.18, 133.82, 129.78, 129.15, 128.43, 128.38, 128.05, 127.83, 125.62, 122.09, 121.84, 121.09, 117.98, 112.99, 103.97 (pyrazole C_4), 72.09 (OCH_2); ESI-MS (*m/z*): 510 $[M+H]^+$, 511 $[M+2]^+$; Anal. Calcd. for $C_{29}H_{23}ClN_4O_2$: C, 70.37; H, 4.68; N, 11.32; Found: C, 70.41; H, 4.61; N, 11.28.

*4.1.3.2. 1-[4-[5-(4-(Benzyloxy)phenyl)-1-(3-chlorophenyl)-1H-pyrazol-3-yl]phenyl]urea (**3b**).* Yield 58%; mp 192–193 °C; IR (cm^{-1}, KBr): 3344 (N-H), 3038 (C-H), 1656 (CONH), 1592 (C=N); ^{1}H NMR (DMSO-d_6): δ 10.13 (s, 1H, CONH, D_2O exchangeable), 7.38–8.07 (m, 17H, Ar-H), 7.05 (s, 1H, pyrazole-H-4), 6.16 (s, 2H, NH_2, D_2O exchangeable), 5.15 (s, 2H, OCH_2); ^{13}C NMR (DMSO-d_6): δ 171.83 (C=O), 160.83 (pyrazole C_3), 159.07 (pyrazole C_5), 151.52, 144.65, 138.27, 136.93, 136.48, 134.72, 130.45, 130.18, 128.90, 128.73, 128.67, 128.42, 125.13, 123.58, 122.38, 121.27, 119.83, 113.79, 105.38 (pyrazole C_4), 71.49 (OCH_2); ESI-MS (*m/z*): 510 $[M+H]^+$, 511 $[M+2]^+$; Anal. Calcd. for $C_{29}H_{23}ClN_4O_2$: C, 70.37; H, 4.68; N, 11.32; Found: C, 70.32; H, 4.63; N, 11.36.

*4.1.3.3. 1-[4-[5-(4-(Benzyloxy)phenyl)-1-(4-chlorophenyl)-1H-pyrazol-3-yl]phenyl]urea (**3c**).* Yield 62%; mp 210–211 °C; IR (cm^{-1}, KBr): 3345 (N-H), 3035 (C-H), 1631 (CONH), 1595 (C=N); ^{1}H NMR (DMSO-d_6): δ 10.25 (s, 1H, CONH, D_2O exchangeable), 7.42–8.09 (m, 17H, Ar-H), 7.07 (s, 1H, pyrazole-H-4), 6.19 (s, 2H, NH_2, D_2O exchangeable), 5.16 (s, 2H, OCH_2); ^{13}C NMR (DMSO-d_6): δ 170.21 (C=O), 159.67 (pyrazole C_3), 158.12 (pyrazole C_5), 151.36, 143.25, 138.31, 136.72, 136.16, 135.94, 130.19, 129.87, 128.97, 128.83, 128.58, 128.14, 125.66, 122.93, 122.62, 120.93, 117.61, 113.18, 104.75 (pyrazole C_4), 70.56 (OCH_2); ESI-MS (*m/z*): 510 $[M+H]^+$, 511 $[M+2]^+$; Anal. Calcd. for $C_{29}H_{23}ClN_4O_2$: C, 70.37; H, 4.68; N, 11.32; Found: C, 70.39; H, 4.72; N, 11.39.

*4.1.3.4. 1-[4-[5-(4-(Benzyloxy)phenyl)-1-(3,4-dichlorophenyl)-1H-pyrazol-3-yl]phenyl]urea (**3d**).* Yield 62%; mp 253–254 °C; IR (cm^{-1}, KBr): 3348 (N-H), 3031 (C-H), 1629 (C=O), 1596 (C=N); ^{1}H NMR (DMSO-d_6): δ 10.25 (s, 1H, CONH, D_2O

exchangeable), 7.42–8.09 (m, 16H, Ar-H), 7.07 (s, 1H, pyrazole-H-4), 6.15 (s, 2H, NH_2, D_2O exchangeable), 5.16 (s, 2H, OCH_2); ^{13}C NMR (DMSO-d_6): δ 171.65 (C=O), 160.29 (pyrazole C_3), 159.05 (pyrazole C_5), 152.07, 144.37, 138.16, 136.54, 136.37, 135.12, 130.86, 130.65, 128.34, 128.14, 128.11, 128.06, 124.95, 123.61, 122.98, 122.65, 119.57, 114.06, 104.32 (pyrazole C_4), 71.32 (OCH_2); ESI-MS (*m/z*): 544 $[M+H]^+$, 545 $[M+2]^+$; Anal. Calcd. for $C_{29}H_{22}Cl_2N_4O_2$: C, 65.79; H, 4.19; N, 10.58; Found: C, 65.84; H, 4.22; N, 10.64.

*4.1.3.5. 1-[4-[5-(4-(benzyloxy)phenyl)-1-(4-fluorophenyl)-1H-pyrazol-3-yl]phenyl]urea (**3e**).* Yield 66%; mp 261–262 °C; IR (cm^{-1}, KBr): 3356 (N-H), 3032 (C-H), 1631 (C=O), 1585 (C=N); ^1H NMR (DMSO-d_6): δ 10.44 (s, 1H, CONH, D_2O exchangeable), 7.49–8.16 (m, 17H, Ar-H), 7.14 (s, 1H, pyrazole-H-4), 6.19 (s, 2H, NH_2, D_2O exchangeable), 5.23 (s, 2H, OCH_2); ^{13}C NMR (DMSO-d_6): δ 170.34 (C=O), 159.21 (pyrazole C_3), 158.36 (pyrazole C_5), 152.65, 144.16, 138.51, 135.43, 135.23, 134.86, 129.65, 129.12, 128.95, 128.63, 128.44, 127.09, 124.07, 123.54, 121.58, 120.87, 118.43, 114.17, 104.69 (pyrazole C_4), 71.62 (OCH_2); ESI-MS (*m/z*): 494 $[M+H]^+$; Anal. Calcd. for $C_{29}H_{23}FN_4O_2$: C, 72.79; H, 4.84; N, 11.71; Found: C, 72.76; H, 4.90; N, 11.77.

*4.1.3.6. 1-[4-[5-(4-(Benzyloxy)phenyl)-1-(3-chloro-4-fluorophenyl)-1H-pyrazol-3-yl]phenyl] urea (**3f**).* Yield 63%; mp 220–221 °C; IR (cm^{-1}, KBr): 3351 (N-H), 3033 (C-H), 1632 (C=O), 1590 (C=N); ^1H NMR (DMSO-d_6): δ 10.21 (s, 1H, CONH, D_2O exchangeable), 7.42–7.82 (m, 16H, Ar-H), 7.10 (s, 1H, pyrazole-H-4), 6.13 (s, 2H, NH_2, D_2O exchangeable), 5.16 (s, 2H, OCH_2); ^{13}C NMR (DMSO-d_6): δ 170.69 (C=O), 159.54 (pyrazole C_3), 158.79 (pyrazole C_5), 151.94, 144.72, 138.09, 135.17, 135.10, 134.94, 129.89, 129.13, 128.82, 128.78, 128.52, 128.17, 124.37, 123.16, 122.43, 120.96, 117.65, 112.65, 105.66 (pyrazole C_4), 72.11 (OCH_2); ESI-MS (*m/z*): 528 $[M+H]^+$, 529 $[M+2]^+$; Anal. Calcd. for $C_{29}H_{22}ClFN_4O_2$: C, 67.90; H, 4.32; N, 10.92; Found: C, 67.84; H, 4.39; N, 10.95.

*4.1.3.7. 1-[4-[5-(4-(Benzyloxy)phenyl)-1-(4-bromophenyl)-1H-pyrazol-3-yl]phenyl]urea (**3g**).* Yield 68%; mp 230–231 °C; IR (cm^{-1}, KBr): 3357 (N-H), 3031 (C-H), 1626 (C=O), 1590 (C=N); ^1H NMR (DMSO-d_6): δ 10.15 (s, 1H, CONH, D_2O exchangeable), 7.42–7.87 (m, 17H, Ar-H), 7.05 (s, 1H, pyrazole-H-4), 6.23 (s, 2H, NH_2, D_2O exchangeable), 5.16 (s, 2H, OCH_2); ^{13}C NMR (DMSO-d_6): δ 171.17 (C=O), 160.62 (pyrazole C_3), 158.12 (pyrazole C_5), 151.39, 144.51, 137.62, 136.15, 135.82, 134.15, 130.65, 130.09, 128.73, 128.65, 128.32, 127.85, 125.62, 123.65, 121.54, 120.32, 118.58, 112.29, 103.81 (pyrazole C_4), 72.18 (OCH_2); ESI-MS (*m/z*): 554 $[M+H]^+$, 555 $[M+2]^+$; Anal. Calcd. for $C_{29}H_{23}BrN_4O_2$: C, 64.57; H, 4.30; N, 10.39; Found: C, 64.53; H, 4.37; N, 10.44.

*4.1.3.8. 1-[4-[5-(4-(Benzyloxy)phenyl)-1-(4-nitrophenyl)-1H-pyrazol-3-yl]phenyl]urea (**3H**).* Yield 61%; mp 215–216 °C; IR (cm^{-1}, KBr): 3341 (N-H), 3030 (C-H), 1631 (C=O), 1590 (C=N); ^1H NMR (DMSO-d_6): δ 10.25 (s, 1H, CONH, D_2O exchangeable), 7.42–8.09 (m, 17H, Ar-H), 7.05 (s, 1H, pyrazole-H-4), 6.12 (s, 2H, NH_2, D_2O exchangeable), 5.16 (s, 2H, OCH_2); ^{13}C NMR (DMSO-d_6): δ 171.39 (C=O), 161.15 (pyrazole C_3), 157.37 (pyrazole C_5), 150.62, 143.09, 137.37, 136.12, 136.09, 135.26, 130.73, 129.08, 128.57, 128.42, 128.13, 128.08, 125.37, 123.19, 122.64, 120.43, 118.43, 112.89, 103.07 (pyrazole C_4), 70.34 (OCH_2); ESI-MS (*m/z*): 521 $[M+H]^+$; Anal. Calcd. for $C_{29}H_{23}N_5O_4$: C, 68.90; H, 4.59; N, 13.85; Found: C, 68.98; H, 4.62; N, 13.91.

*4.1.3.9. 1-[4-[5-(4-(Benzyloxy)phenyl)-1-(2,4-dinitrophenyl)-1H-pyrazol-3-yl]phenyl]urea (**3i**).* Yield 64%; mp 222–223 °C; IR (cm^{-1}, KBr): 3624, 3346 (N-H), 3031 (C-H), 1626 (C=O), 1585 (C=N); ^1H NMR (DMSO-d_6): δ 10.39 (s, 1H, CONH, D_2O exchangeable), 7.42–7.88 (m, 16H, Ar-H), 7.05 (s, 1H, pyrazole-H-4), 6.20 (s, 2H, NH_2, D_2O exchangeable), 5.16 (s, 2H, OCH_2); ^{13}C NMR (DMSO-d_6): δ 170.74 (C=O), 160.37 (pyrazole C_3), 157.95 (pyrazole C_5), 150.38, 142.96, 138.65, 136.09, 135.26, 134.09, 130.56, 129.13, 128.97, 128.32, 128.05, 127.57, 124.92, 123.42, 121.90, 120.56, 119.37, 112.48, 102.48 (pyrazole C_4), 70.19 (OCH_2); ESI-MS (*m/z*): 566 $[M+H]^+$; Anal. Calcd. for $C_{29}H_{22}N_6O_6$: C, 63.27; H, 4.03; N, 15.27; Found: C, 63.33; H, 4.09; N, 15.20.

*4.1.3.10. 1-[4-[5-(4-(Benzyloxy)phenyl)-1-(2-methylphenyl)-1H-pyrazol-3-yl]phenyl]urea (**3j**).* Yield 57%; mp 200–201 °C; IR (cm^{-1}, KBr): 3632, 3347 (N-H), 3029 (C-H), 1639 (C=O), 1588 (C=N); ^1H NMR (DMSO-d_6): δ 10.25 (s, 1H, CONH, D_2O exchangeable), 7.42–7.83 (m, 17H, Ar-H), 7.05 (s, 1H, pyrazole-H-4), 6.22 (s, 2H, NH_2, D_2O exchangeable), 5.10 (s, 2H, OCH_2), 2.06 (s, 3H, CH_3); ^{13}C NMR (DMSO-d_6): δ 170.11 (C=O), 160.96 (pyrazole C_3), 158.07 (pyrazole C_5), 152.77, 142.08, 138.14, 136.02, 135.87, 135.13, 130.75, 129.62, 128.59, 128.32, 128.17, 127.27, 124.85, 122.96, 121.87, 120.61, 119.01, 114.83, 103.67 (pyrazole C_4), 72.54 (OCH_2), 17.83 (CH_3); ESI-MS (*m/z*): 490 $[M+H]^+$; Anal. Calcd. for $C_{30}H_{26}N_4O_2$: C, 75.93; H, 5.52; N, 11.81; Found: C, 75.85; H, 5.59; N, 11.76.

*4.1.3.11. 1-[4-[5-(4-(Benzyloxy)phenyl)-1-(3-methylphenyl)-1H-pyrazol-3-yl]phenyl]urea (**3k**).* Yield 55%; mp 202–203 °C; IR (cm^{-1}, KBr): 3635, 3350 (N-H), 3037 (C-H), 1635 (C=O), 1592 (C=N); ^1H NMR (DMSO-d_6): δ 10.25 (s, 1H, CONH, D_2O exchangeable), 7.42–7.81 (m, 17H, Ar-H), 7.05 (s, 1H, pyrazole-H-4), 6.14 (s, 2H, NH_2, D_2O exchangeable), 5.11 (s, 2H, OCH_2), 2.06 (s, 3H, CH_3); ^{13}C NMR (DMSO-d_6): δ 170.35 (C=O), 161.48 (pyrazole C_3), 159.53 (pyrazole C_5), 152.09, 143.73, 138.95, 135.47, 135.05, 134.85, 129.86, 129.15, 128.83, 128.48, 128.39, 128.11, 125.16, 122.58, 121.74, 120.13, 117.46, 114.61, 104.17 (pyrazole C_4), 71.56 (OCH_2), 17.18 (CH_3); ESI-MS (*m/z*): 490 $[M+H]^+$; Anal. Calcd. for $C_{30}H_{26}N_4O_2$: C, 75.93; H, 5.52; N, 11.81; Found: C, 75.96; H, 5.55; N, 11.87.

*4.1.3.12. 1-[4-[5-(4-(Benzyloxy)phenyl)-1-(4-methylphenyl)-1H-pyrazol-3-yl]phenyl]urea (**3l**).* Yield 60%; mp 215–216 °C; IR (cm^{-1}, KBr): 3613, 3358 (N-H), 3031 (C-H), 1635 (C=O), 1585 (C=N); ^1H NMR (DMSO-d_6): δ 10.39 (s, 1H, CONH, D_2O exchangeable), 7.36–7.91 (m, 17H, Ar-H), 7.05 (s, 1H, pyrazole-H-4), 6.12 (s, 2H, NH_2, D_2O exchangeable), 5.22 (s, 2H, OCH_2), 2.12 (s, 3H, CH_3); ^{13}C NMR (DMSO-d_6): δ 171.49 (C=O), 160.55 (pyrazole C_3), 159.66 (pyrazole C_5), 151.08, 143.02, 138.54, 135.39, 135.17, 135.06, 130.52, 129.34, 128.72, 128.65, 128.43, 128.31, 125.08, 123.81, 121.31, 120.07, 117.32, 113.35, 105.04 (pyrazole C_4), 71.97 (OCH_2), 17.66 (CH_3); ESI-MS (*m/z*): 490 $[M+H]^+$; Anal. Calcd. for $C_{30}H_{26}N_4O_2$: C, 75.93; H, 5.52; N, 11.81; Found: C, 75.97; H, 5.48; N, 11.83.

*4.1.3.13. 1-[4-[5-(4-(Benzyloxy)phenyl)-1-(2,6-dimethylphenyl)-1H-pyrazol-3-yl]phenyl]urea (**3m**).* Yield 68%; mp 213–214 °C; IR (cm^{-1}, KBr): 3628, 3349 (N-H), 3037 (C-H), 1635 (C=O), 1592 (C=N); ^1H NMR (DMSO-d_6): δ 10.21 (s, 1H, CONH, D_2O

exchangeable), 7.42–7.80 (m, 16H, Ar-H), 7.05 (s, 1H, pyrazole-H-4), 6.18 (s, 2H, NH_2, D_2O exchangeable), 5.12 (s, 2H, OCH_2), 2.11 (s, 6H, CH_3); ^{13}C NMR (DMSO-d_6): δ 171.96 (C=O), 160.91 (pyrazole C_3), 159.27 (pyrazole C_5), 152.56, 143.95, 137.53, 135.91, 135.08, 134.73, 129.31, 129.06, 128.56, 128.52, 128.37, 128.08, 125.37, 123.49, 122.06, 120.95, 118.78, 113.47, 105.25 (pyrazole C_4), 71.82 (OCH_2), 17.53 (2 CH3); ESI-MS (*m/z*): 489 $[M+H]^+$; Anal. Calcd. for $C_{31}H_{28}N_4O_2$: C, 76.21; H, 5.78; N, 11.47; Found: C, 76.18; H, 5.71; N, 11.42.

*4.1.3.14. 1-[4-[5-(4-(Benzyloxy)phenyl)-1-(2-methoxyphenyl)-1H-pyrazol-3-yl]phenyl]urea (**3n**).* Yield 55%; mp 240–241 °C; IR (cm^{-1}, KBr): 3633, 3353 (N-H), 3029 (C-H), 1621 (C=O), 1595 (C=N); ^1H NMR (DMSO-d_6): δ 10.23 (s, 1H, CONH, D_2O exchangeable), 7.42–7.86 (m, 17H, Ar-H), 7.05 (s, 1H, pyrazole-H-4), 6.23 (s, 2H, NH_2, D_2O exchangeable), 5.18 (s, 2HH, OCH_2), 3.72 (s, 3H, OCH_3); ^{13}C NMR (DMSO-d_6): δ 170.27 (C=O), 159.76 (pyrazole C_3), 151.32 (pyrazole C_5), 143.01, 137.08, 134.96, 134.01, 133.12, 133.01, 130.63, 129.27, 128.87, 128.75, 128.69, 128.57, 125.36, 123.16, 122.53, 121.28, 118.03, 113.26, 105.68 (pyrazole C_4), 70.65 (OCH_2), 56.81 (OCH_3); ESI-MS (*m/z*): 491 $[M+H]^+$; Anal. Calcd. for $C_{30}H_{26}N_4O_3$: C, 73.45; H, 5.34; N, 11.42; Found: C, 73.41; H, 5.28; N, 11.47.

*4.1.3.15. 1-[4-[5-(4-(Benzyloxy)phenyl)-1-(4-methoxyphenyl)-1H-pyrazol-3-yl]phenyl]urea (**3o**).* Yield 61%; mp 243–244 °C; IR (cm^{-1}, KBr): 3345 (N-H), 3032 (C-H), 1673 (CONH), 1590 (C=N); ^1H NMR (DMSO-d_6): δ 10.55(s, 1H, CONH, D_2O exchangeable), 7.42–7.91 (m, 17H, Ar-H), 7.05 (s, 1H, pyrazole-H-4), 6.21 (s, 2H, NH_2, D_2O exchangeable), 5.21 (s, 2H, OCH_2), 3.74 (s, 3H, OCH_3); ^{13}C NMR (DMSO-d_6): δ 170.68 (C=O), 159.63 (pyrazole C_3), 152.61 (pyrazole C_5), 143.68, 138.82, 134.62, 134.13, 134.06, 133.65, 130.54, 129.09, 128.75, 128.63, 128.51, 127.28, 124.19, 123.47, 122.01, 121.79, 119.12, 113.54, 103.21 (pyrazole C_4), 72.05 (OCH_2), 56.39 (OCH_3); ESI-MS (*m/z*): 491 $[M+H]^+$; Anal. Calcd. for $C_{30}H_{26}N_4O_3$: C, 73.45; H, 5.34; N, 11.42; Found: C, 74.38; H, 5.37; N, 11.46.

4.2. *Pharmacology*

p38α MAPK assay was performed using the CycLex p38 Kinase assay kit (Cat CY-1177) procured from MBL, USA. CycLex p38α positive control (Cat CY-E1177) was also purchased from MBL, USA. The commercially available ELISA kit (Cat KB2052, Krishgen Biosystems, Mumbai, India) was used for TNF-α estimation in the mice plasma samples. LPS from *Escherichia coli* 0111:B4 (Cat 9028) was obtained from Chondrex, USA. All the pharmacological experiments were conducted in compliance with ethical principles after Institutional Animal Ethics Committee (IAEC, No. 173/CPCSEA, 2000) approval. Animals were obtained from central animal house facility, Hamdard University, New Delhi. The experiments were performed in albino rats of Wistar strain of either sex, weighing 180–200 g. The animals were maintained at 25 ± 2 °C, 50 ± 5% relative humidity and 12 h light/dark cycle. Food and water were freely available up to the time of experiments.

4.2.1. *p38α MAPK assay*

Inhibition of p38α MAPK activity was determined according to the method of Forrer et al.[25]. All the samples were diluted with a kinase buffer as needed. In the test sample wells kinase reaction buffer (80 µL) and 10 × inhibitor compounds or standard (SB 203580) (10 µL) were added. In the solvent control experiment, 80 µL of kinase reaction buffer and 10 µL of solvent for inhibitor were added. In the inhibition control wells, 80 µL of kinase reaction buffer and 10 µL of 10 × SB 203580 (20 µmol/L) were added. The reaction in all wells was initiated by adding 10 µL of p38α positive control to each well and mixing thoroughly at room temperature. The plate was covered and incubated at 30 °C for 30 min. The wells were washed five times with a wash buffer. 100 µL of anti-phospho-ATF-2 Thr71 polyclonal antibody PPT-09 was pipetted into each well, covered and incubated at room temperature for 30 min. The wells were washed five times with a wash buffer. HRP-conjugated anti-rabbit IgG (100 µL) was pipetted into each well, covered and incubated at room temperature for 30 min. The wells were washed five times with a wash buffer. 100 µL of substrate reagent (tetramethylbenzidine, TMB) was added to each well and incubated at room temperature for 5–15 min. Finally 100 µL of a stop solution (1 mol/L H_2SO_4) was added to each well and absorbance was measured in each well using a spectrophotometric plate reader at a wavelength of 450 nm. IC_{50} values were calculated. All samples were assayed in triplicates.

4.2.2. *Antioxidant assay*

All the compounds (**3a–o**) were evaluated for their *in vitro* free radical scavenging activity by the 2,2′-diphenyl-1-picrylhydrazyl (DPPH) radical scavenging method described by Blois et al.[26].

4.2.3. *Anti-inflammatory activity*

Compounds **3a–e, 3g** and **3h** were evaluated for their anti-inflammatory activity by the carrageenan-induced rat paw edema method of Winter et al.[27] using Digital Plethysmometer-PLM-01 Plus (Orchid Scientifics and Innovatives India Pvt., Ltd., Mumbai, India).

4.2.4. *Ulcerogenic test and lipid peroxidation*

The most active compound of the series **3a–e, 3g** and **3h** were evaluated for their ulcerogenic potential in rats by already reported procedure[28,29]. Lipid peroxidation in the gastric mucosa was determined according to the already reported method of Ohkawa et al.[30].

4.2.5. *TNF-α production inhibition evaluation*

TNF-α production inhibition in mice (BALB/c) weighing 20–30 g was carried out using the already reported procedure[31,32].

4.2.6. *Molecular docking study*

To analyze the biological activity on the basis of structure, molecular docking studies of the compounds were carried out by taking X-ray crystal structure data to establish the interactions of the compounds with the p38α MAPK (PDB code: 3D83 having resolution of 1.90 Å). The molecular docking study was used to understand the possible best binding pose of compounds (**3a–o**) by which it could be sorted out for identifying promising p38α MAPK inhibitor using Glide extra precision (XP) Maestro 10.1 Schrodinger, (2015-Release-4) running on the Linux 64 operating system[33]. Molecular docking studies mainly involve selection and preparation of appropriate protein, grid generation, ligand preparation followed by docking and analysis. The ligands and the receptors were prepared using the LigPrep and Protein preparation

wizard, respectively. Missing hydrogens were added using prime and unwanted water molecules were also removed.

4.3. Statistical analysis

Results are expressed as the mean ± SEM (standard error of the mean) of six animals per group. The data obtained from pharmacological experiments were analyzed using the Student's *t*- test. A *P* value of less than 0.05 was considered statistically significant.

Acknowledgments

The authors are thankful to In-charge Animal House for providing animals and In-charge, Central Instrumentation Facility (CIF) for spectral analysis of compounds. The authors also thank Dr. Ozair Alam, Assistant Professor in the Department of Pharmaceutical Chemistry, Hamdard University, for carrying out docking studies. One of the authors (Kanagasabai Somakala) is grateful to Department of Science and Technology, Women Scientists Scheme-A (File No. SR/WOS-A/CS-84/2013), New Delhi, for providing financial assistance.

Appendix A. Supporting information

Supplementary data associated with this article can be found in the online version at http://dx.doi.org/10.1016/j.apsb.2016.08.006.

References

1. R. Medzhitov, Inflammation: new adventures of an old flame, Cell **140**, 2010, 771-776.
2. Bacchi S, Palumbo P, Sponta A, Coppolino MF. Clinical pharmacology of non-steroidal anti-inflammatory drugs: a review. *Antiinflamm Antiallergy Agents Med Chem* 2012;**11**:52–64.
3. Rubio-Perez JM, Morillas-Ruiz JM. A review: inflammatory process in Alzheimer's disease, role of cytokines. *Sci World J* 2012;**2012**:756357.
4. Vane JR, Botting RM. Anti-inflammatory drugs and their mechanism of action. *Inflamm Res* 1998;**47**:78–87.
5. Xie WL, Chipman JG, Robertson DL, Erikson RL, Simmons DL. Expression of a mitogen-responsive gene encoding prostaglandin synthase is regulated by mRNA splicing. *Proc Natl Acad Sci USA* 1991;**88**:2692–6.
6. Kujubu DA, Fletcher BS, Varnum BC, Lim RW, Herschman HR. TIS10, a phorbol ester tumor promoter-inducible mRNA from Swiss 3T3 cells, encodes a novel prostaglandin synthase/cyclooxygenase homologue. *J Biol Chem* 1991;**266**:12866–72.
7. Dannhardt G, Kiefer W. Cyclooxygenase inhibitors-current status and future prospects. *Eur J Med Chem* 2001;**36**:109–26.
8. Stillman MJ, Stillman MT. Choosing nonselective NSAIDs and selective COX-2 inhibitors in the elderly. A clinical use pathway. *Geriatrics* 2007;**62**:26–34.
9. Chakravarty S, Dugar S. Inc. Chapter 18. Inhibitors of p38α MAP kinase. *Annu Rep Med Chem* 2002;**37**:177–86.
10. Amir M, Somakala K, Ali S. p38 MAP kinase inhibitors as anti inflammatory agents. *Min Rev Med Chem* 2013;**13**:2082–96.
11. Chen Z, Gibson TB, Robinson F, Silvestro L, Pearson G, Xu B, et al. MAP kinases. *Chem Rev* 2001;**101**:2449–76.
12. Badger AM, Bradbeer JN, Votta B, Lee JC, Adams JL, Griswold DE. Pharmacological profile of SB 203580, a selective inhibitor of cytokine suppressive binding protein/p38 kinase, in animal models of arthritis, bone resorption, endotoxin shock and immune function. *J Pharmacol Exp Ther* 1996;**279**:1453–61.
13. Smith RJ. Therapies for rheumatoid arthritis: hope springs eternal. *Drug Discov Today* 2005;**10**:1598–606.
14. Sticherling M. Mechanisms of psoriasis. *Drug Discov Today: Dis Mech* 2005;**2**:275–81.
15. Locksley RM, Killeen N, Lenardo MJ. The TNF and TNF receptor superfamilies: integrating mammalian biology. *Cell* 2001;**104**:487–501.
16. Xanthoulea S, Pasparakis M, Kousteni S, Brakebusch C, Wallach D, Bauer J, et al. Tumor necrosis factor (TNF) receptor shedding controls thresholds of innate immune activation that balance opposing TNF functions in infectious and inflammatory diseases. *J Exp Med* 2004;**200**:367–76.
17. Zhou Y, Liu J, Zheng MY, Zheng SL, Jiang CY, Zhou XM, et al. Structural optimization and biological evaluation of 1, 5-disubstituted pyrazole-3-carboxamines as potent inhibitors of human 5-lipoxygenase. *Acta Pharm Sin B* 2016;**6**:32–45.
18. Keche AP, Hatnapure GD, Tale RH, Rodge AH, Kamble VM. Synthesis, anti-inflammatory and antimicrobial evaluation of novel 1-acetyl-3, 5-diaryl-4, 5-dihydro (1*H*) pyrazole derivatives bearing urea, thiourea and sulfonamide moieties. *Bioorg Med Chem Lett* 2012;**22**:6611–5.
19. Moss N, Breitfelder S, Betageri R, Cirillo PF, Fadra T, Hickey ER, et al. New modifications to the area of pyrazole-naphthyl urea based p38 MAP kinase inhibitors that bind to the adenine/ATP site. *Bioorg Med Chem Lett* 2007;**17**:4242–7.
20. Regan J, Capolino A, Cirillo PF, Gilmore T, Graham AG, Hickey E, et al. Structure-activity relationships of the p38α MAP kinase inhibitor 1-(5-*tert*-butyl-2-*p*-tolyl-2*H*-pyrazol-3-yl)-3-[4-(2-morpholin-4-yl-ethoxy)naph-thalen-1-yl]urea (BIRB 796). *J Med Chem* 2003;**46**:4676–86.
21. Amir M, Kumar H, Javed SA. Condensed bridgehead nitrogen heterocyclic system: synthesis and pharmacological activities of 1, 2, 4-triazolo-[3, 4-*b*]-1, 3, 4-thiadiazole derivatives of ibuprofen and biphenyl-4-yloxy acetic acid. *Eur J Med Chem* 2008;**43**:2056–66.
22. Amir M, Saifullah K, Akhter W. Design, synthesis and pharmacological evaluation of novel azole derivatives of aryl acetic acid as anti-inflammatory and analgesic agents. *J Enzym Inhib Med Chem* 2011;**26**:141–8.
23. Amir M, Akhter MW, Alam O. Synthesis, characterization, and biological evaluation of furoxan coupled ibuprofen derivatives as anti-inflammatory agents. *Monatsh Chem* 2016;**147**:493–508.
24. Somakala K, Amir M, Sharma V, Wakode S. Synthesis and pharmacological evaluation of pyrazole derivatives containing sulfonamide moiety. *Monatsh Chem* 2016. Available from: http://dx.doi.org/10.1007/s00706-016-1694-x.
25. Forrer P, Tamaskovic R, Jaussi R. Enzyme-linked immunosorbent assay for measurement of JNK, ERK, and p38 kinase activities. *Biol Chem* 1998;**379**:1101–11.
26. Blois MS. Antioxidant determination by the use of a stable free radical. *Nature* 1958;**181**:1119–200.
27. Winter CA, Risely EA, Nuss GM. Carrageenin-induced edema in hind paw of the rat as an assay for antiinflammatory drugs. *Exp Biol Med* 1962;**111**:544–7.
28. Bekhit AA, Fahmy HT, Rostom SA, Bekhit AE. Synthesis and biological evaluation of some thiazolylpyrazole derivatives as dual anti-inflammatory antimicrobial agents. *Eur J Med Chem* 2010;**45**:6027–38.
29. Cioli V, Putzolu S, Rossi V, Sorza Barcellona P, Corradino C. The role of direct tissue contact in the production of gastrointestinal ulcers by anti-inflammatory drugs in rats. *Toxicol Appl Pharmacol* 1979;**50**:283–9.
30. Ohkawa H, Ohishi N, Yagi K. Assay for lipid peroxides in animal tissues by thiobarbituric acid reaction. *Anal Biochem* 1979;**95**:351–8.
31. Griswold DE, Hilegass LM, O'Leary-Bartus L, Lee JC, Laydon JT, Trophy TJ. Evaluation of human cytokine production and effects of

pharmacological agents in a heterologous system *in vivo*. *J Immunol Methods* 1996;**195**:1–5.
32. Nakao A, Ohkawa N, Nagasaki T, Kagari T, Doi H, Shimozato T, et al. Tetrahydropyridine derivatives with inhibitory activity on the production of proinflammatory cytokines: part 1. *Bioorg Med Chem Lett* 2009;**19**:4607–10.
33. Maestro V, Schrodinger LLC. *Maestro, version 10.1*. New York, NY: Schrödinger LLC; 2015.